ARTICLE

BcRISP1, isolated from non-heading Chinese cabbage, decreases the seed set of transgenic *Arabidopsis*

Tongkun Liu[1,2,3,*], Yu Qian[1,2,3,*], Weike Duan[1,2,3], Jun Ren[1,2,3], Xilin Hou[1,2,3] and Ying Li[1,2,3]

Mitochondria are the energy sources of plant cells and are involved in regulating cell development. Ubiquinol–cytochrome c reductase iron-sulfur protein, which is necessary for mitochondrial respiration, is a subunit of mitochondrial electron transport chain multimeric enzyme complexes. To better understand the biological function of the ubiquinol–cytochrome c reductase iron–sulfur protein, the full-length cDNA of *BcRISP1* was cloned; it was found to contain 810 base pairs and encode 269 amino acids. Unusually, high expression of the *BcRISP1* gene in the archesporial cell stages was determined by quantitative reverse transcription-polymerase chain reaction (qRT-PCR) analysis of cytoplasmic male sterile lines and maintainer lines. The seed set was affected by the overexpression of *BcRISP1*, and shorter siliques with lower seed sets were observed in 35S::*BcRISP1 Arabidopsis* plants. These characteristics may have resulted from the reduced formation of pollen and impaired pollen tube growth. qRT-PCR results revealed that in 35S::*BcRISP1* plants, the expression levels of the mitochondrial respiratory chain-related genes, *COX10* and *RIP1*, were enhanced, whereas the expression levels of *QCR7* and *SDH2-1* were reduced. This result implies that overexpression of *BcRISP1* in transgenic *Arabidopsis* plants may disrupt the mitochondrial electron transport chain by affecting the expression of mitochondrial respiratory chain-related genes and therefore, reducing the seed set.

Horticulture Research (2014) **1,** 14062; doi:10.1038/hortres.2014.62; Published online: 10 December 2014

INTRODUCTION

In flowering plants, the male gametophyte or pollen grain is a multi-celled life unit. Pollen formation is high in energy consumption, involving several layers of cells that enclose a fluidic locule, within which microspores mature to become pollen grains.[1–4] In this process, the germ cells in an anther primordium first divide into pollen mother cells, which then undergo meiosis and produce haploid microspores. In developing pollen grains, energy is exclusively supplied by mitochondria in non-photosynthetic tissues without differentiated plastids and amyloplasts.[5] Therefore, mitochondrial dysfunction in pollen grains has a drastic impact upon pollen development.[6]

Mitochondria are central to the regulation of cellular energy homeostasis and redox balance and have been shown to bear the causal defect in some cytoplasmic male sterility (CMS) species. The mitochondrial electron transport chain consists of four major multimeric enzyme complexes, one of which is the ubiquinol–cytochrome c oxidoreductase, which is commonly referred to as the cytochrome $bc1$ complex or complex III.[7] All bcl complexes contain a core of three catalytic subunits: cytochrome b, which has two heme groups; cytochrome cl; and the Rieske iron–sulfur protein (RISP), which contains a non-heme 2Fe-2s cluster.[8] Complex III is the central segment of energy-conservation, the mitochondria electron transfer chain, and has many respiratory functions.[9] In this cycle, it is proposed that RISP transfers an electron from a reduced quinol to cytochrome $c1$; this is consistent with the ubisemiquinone generation site being a substrate for cytochrome b.[8] Reconstitution experiments and genetic analysis have shown that RISP is absolutely necessary for mitochondrial respiration.[10,11]

In plants, cytoplasmic male sterility (CMS) is a widespread phenotypic trait that characterizes a plant's inability to produce viable pollen.[12] Approximately 10 types of CMS have been identified in *Brassica*, with Pol CMS being one of the most widely used for investigations of CMS function and mechanisms.[13] In our preliminary study on Pol CMS in non-heading Chinese cabbage (*Brassica campestris* ssp. *chinensis* Makino), suppression subtractive hybridization revealed one expressed sequence tag, annotated as Rieske iron–sulfur protein (named *BcRISP1*), which was highly expressed in the sterile line (Pol CMS) of non-heading Chinese cabbage compared to the maintainer line.

The objective of this study was to determine the physiological role of this protein. We evaluated the function of *BcRISP1* in non-heading Chinese cabbage using quantitative reverse transcription-PCR (qRT-PCR) and ectopic expression in *Arabidopsis*. This study will contribute to an improved understanding of the molecular basis of pollen development in non-heading Chinese cabbage.

MATERIALS AND METHODS

Plant materials, growth conditions and treatments

Pol CMS and maintainer plants of non-heading Chinese cabbage (*Brassica campestris* ssp. *chinensis* Makino) were grown in a greenhouse under a light/dark cycle of 16 h light/8 h dark at 24/16℃.

Wild-type *A. thaliana* (Columbia ecotype) and *BcRISP1* overexpressing *A. thaliana* plants were used in this study. Seeds were incubated in environmentally controlled growth chambers at 23/18 ℃ day/night under 60% relative humidity. Cool white fluorescent lights supplied photons at 120 μmol m^{-2} s^{-1} with a 16 h light and 8 h dark photoperiod.

Amplification and cloning of *BcRISP1* cDNAs

A *BcRISP1* expressed sequence tag was identified in a forward subtractive cDNA library that was constructed using the suppression subtractive hybridization method with Pol CMS flower cDNA as the tester and cDNA from

maintainer flowers as the driver. The full-length gene was cloned from Pol CMS flowers using homology cloning with a Taq LA DNA polymerase PCR kit (TaKaRa, Dalian, China) with the gene-specific *BcRISP1*F1 and *BcRISP1*R1 primers (Table 1). The resultant fragments were cloned into a pMD18-T vector (TaKaRa) and transformed into the *Escherichia coli* host DH5alpha. Positive transformants were first screened by PCR and then sequenced by the Genscript Biocompany (Nanjing, China).

The above PCR reactions were performed in a 20 μL reaction system containing the following: 1 U Takara Ex Taq, 1× Ex Taq buffer (plus Mg^{2+}), 0.2 mM dNTP mixture, 0.2 mM forward primer, 0.2 mM reverse primer and 1 μL cDNA template. Amplification was performed as follows: initial denaturation (94 ℃, 2 min); 35 cycles of denaturation (94 ℃, 30 s), annealing (52 ℃, 30 s) and extension (72 ℃, 1 min); and final extension (72 ℃, 10 min). All quantitative RT-PCR analyses were performed with iQ5 multicolor real-time PCR detection system (Bio-Rad, Hercules, CA, USA) using 2× SYBR Green SuperMix (170-8882; Bio-Rad). The PCR products were analyzed on 1% agarose gels and extracted using a QIA quick gel extraction kit (Qiagen, Beijing, China).

Bioinformatic analysis
For sequence alignment, gene annotations from different plant species were obtained from the National Center for Biotechnology Information, and BLAST searches were performed to determine the homology of *BcRISP1* DNA sequences. Amino acid sequence homology analysis was performed with Clustal X2, and a phylogenetic tree was constructed with MEGA 5.0 Software using the neighbor-joining method.

Expression analysis
Total RNA was isolated from non-heading Chinese cabbage in different development tissues in the maintainer line (flowers of different sizes (<0.5, 1.5, 2.5 and >3.5 mm) and leaves) and in Pol CMS (flowers of different sizes (<0.6, 1.8, 3.0 and >4.5 mm) and leaves). Polymerase chain reaction was performed for qRT-PCR using *BcRISP1*F2 and *BcRISP1*R2 primers, with *GAPDH* as an internal standard (Table 1). In *Arabidopsis*, total RNA was extracted from the wild-type Columbia ecotype and *BcRISP1* overexpressing transgenic plants using an RNeasy plant mini kit (Qiagen, Beijing, China) according to the manufacturer's instructions. qRT-PCR was performed in 20 μL reaction mixtures containing 10 μL SYBR Premix Ex Taq (2×), 0.4 μL gene forward primer (10 μM), 0.4 μL gene reverse primer (10 μM), 2 μL cDNA and ddH$_2$O up to 20 μL using a CFX96 system (Bio-Rad, Hercules, CA, USA). The qRT-PCR reaction was programmed as follows: pre-denaturation at 94 ℃ for 20 s; and 35 cycles of denaturation at 94 ℃ for 10 s, annealing at 55 ℃ for 20 s and extension at 65 ℃ for 5 s. The comparative C_T value method[14] was used to analyze the *BcRISP1* expression profile. Data were collected at 72 ℃ in each cycle, and the expression levels of the *Arabidopsis* genes were calculated using *TUB2* as the reference gene.[15] The qRT-PCR analysis was

repeated three times, each consisting of three technical replicates. The qRT-PCR primer sequences are provided in Table 1.

Generation of transgenic plants
To express the *BcRISP1* gene in *Arabidopsis*, *BcRISP1* was inserted into the *pEarleyGate103* binary vector as a selectable maker using Gateway Technology (Invitrogen, Carlsbad, USA https://www.invitrogen.com) to construct *pGate-BcRISP1*. The *pGate-BcRISP1* binary vectors were introduced into *Agrobacterium tumefaciens* strain GV3101.

The *A. thaliana* Columbia ecotype was transformed with the *BcRISP1* construct. Flowers were dipped with *A. tumefaciens* GV3101 suspended in 5% sucrose, and the plants were incubated in a growth chamber at 25 ℃ with 100% humidity for 1 day, before transferring to a growth chamber with a 16 h photoperiod at 23 ℃.

Quantification of reactive oxygen species (ROS)
A Reactive Oxygen Species Assay Kit (Beyotime, Nantong, China) was used for ROS quantification. A total of 100 μL of purified mitochondria (100 μg mL^{-1}) and 100 μL of 20 μM dichlorofluorescin diacetate (Molecular Probes, Eugene, OR, USA) in phosphate-buffered saline with dissolved dimethyl sulfoxide, were added to each well of a 96-well microtiter plate. The fluorescent DCF signals, which were produced when dichlorofluorescin diacetate was oxidized by H$_2$O$_2$ and other peroxides, were detected with a multifunctional microplate reader (Infinite M 200; Tecan, Männedorf, Switzerland) by monitoring emissions at 520 nm with an excitation wavelength of 485 nm.[16]

Characterization of *in vitro* pollen tube growth
To examine the pollen grain viability, anthers from mature flowers were dissected and soaked in 0.1% 2,3,5-triphenyl-2h-tetrazolium chloride (TTC) solution. Active pollen grains were stained red because the NADH/NADPH produced deoxidizes TTC to triphenyl methyl hydrazone. The number of pollen grains was counted under a bright field microscope (Axio Imager. A1; Zeiss, Oberkochen, Germany). Pollen germination was performed *in vitro* at 28 ℃ and 100% relative humidity. The pollen grains were cultured on a liquid medium consisting of boric acid (250 mg L^{-1}) and sucrose (10%). From each culture, at least 300 pollen grains were examined to calculate the average germination rate. Pollen germination success was calculated and photographed after 4 h using a bright field microscope (Axio Imager. A1; Zeiss, Oberkochen, Germany).

RESULTS

Cloning and characterization of *BcRISP1*
A full-length cDNA *BcRISP1* clone containing an 810 bp ORF was obtained by PCR amplification using the *BcRISP1*F1 and *BcRISP1*R1

Table 1. Primers used in this study

Gene name	Direction	Sequence (5′–3′)	Use
BcRISP1	F1	ATG CTG CGA ATT GCA GGG A	ORF cloning
	R1	ACC AAT GAG TAA CTT GTT CT	ORF cloning
	F2	GCT ATC AAA ACA CCT AAC TC	For qRT-PCR in non-heading Chinese cabbage
	R2	ATT AGG CAA GGG GAT ACA CC	For qRT-PCR in non-heading Chinese cabbage
	F	AGA TTA TCC CAT CTC CAA T	For qRT-PCR in *Arabidopsis*
	R	AGG CAA AAC CTA ACT CAT	For qRT-PCR in *Arabidopsis*
GAPDH	F	CCA CTA ACT GCC TTG CTC CAC	For qRT-PCR in non-heading Chinese cabbage
	R	GCT TGC CCT CAG ATT CCT CCT	For qRT-PCR in non-heading Chinese cabbage
COX10	F	GCC TTC AGG ACG TAT TAG TG	For qRT-PCR in *Arabidopsis*
	R	TTG ATA GGG TGA AGT TGC TT	For qRT-PCR in *Arabidopsis*
RIP1	F	TTA AAG GAA TAT CCG CAA AG	For qRT-PCR in *Arabidopsis*
	R	ATC TCT GCT CAA ATG GGT TA	For qRT-PCR in *Arabidopsis*
QCR7	F	CTA AGT GGA TAT GTT GCT A	For qRT-PCR in *Arabidopsis*
	R	CTT AAA CGA TTC TGA GAG A	For qRT-PCR in *Arabidopsis*
SDH2-1	F	GCT TGA TGG GAT GTA TGA AT	For qRT-PCR in *Arabidopsis*
	R	GTC GTC AAT AGC CTC AAG TC	For qRT-PCR in *Arabidopsis*
TUB2	F	TCG TCC TAC TTT GTG GAG TGG	For qRT-PCR in *Arabidopsis*
	R	CTC GCC TGA ACA TCT CTT GG	For qRT-PCR in *Arabidopsis*

Abbreviations: F, forward; R, reverse.

Sequence data from this article can be found in the GenBank data library under the *Arabidopsis* accession numbers: *BcRISP1* (not logged), *GAPDH* (AB367451.1), *SDH2-1* (At3g27380), *QCR7* (At4g32470), *COX10* (At2g44520), *RIP1* (At5g13440) and *TUB2* (At5g62690).

primers (Table 1). The calculated mass and theoretical isoelectric point of the putative protein were 67.91 kDa and 4.88, respectively. According to SMART (http://smart.embl-heidelberg.de/) alignment results, this protein contained a ubiquinol cytochrome reductase transmembrane region from Ala[77] to Asp[141] and a Rieske [2Fe–2S] domain from Val[170] to Lys[266] (Figure 1a). The ubiquinol cytochrome reductase transmembrane region is a respiratory subunit and provides a single helix that makes up the transmembrane region of the complex.[17] The Rieske subunit acts by binding with either a ubiquinol or a plastoquinol anion, transferring an electron to the 2Fe–2S cluster, and then releasing the electron to the cytochrome c or cytochrome f heme iron.[18,19]

BcRISP1 homology analysis

Phylogenetic analysis was performed to estimate the structural similarities among non-heading Chinese cabbage *BcRISP1* proteins and ubiquinol–cytochrome c reductase iron–sulfur subunit proteins from other species (Figure 1). The alignment of the *BcRISP1* amino-acid sequences and related proteins from other species was highly conserved (Figure 1a). The phylogenetic tree revealed that

Figure 1. Homology analysis of *BcRISP1*. (**a**) Amino-acid sequence alignment of *BcRISP1* and related proteins from diverse plants. The location of the UCR_TM and Rieske domains in *BcRISP1* was from Ala[77] to Asp[141] and Val[170] to Lys[266], respectively. Sequences were aligned using Clustal X2. (**b**) Phylogenetic analysis of the *BcRISP1* gene. Alignments were based on protein sequences deduced from cDNA or genomic clones. The phylogenetic tree was constructed by MEGA 5.0 software using the neighbor-joining method. Numbers at the nodes represent bootstrap values from 1000 replications. Sequences were obtained from: Bc, *Brassica campestris* ssp. *chinensis* (not logged); Br, *Brassica rapa* ssp. *pekinensis* (Bra006199); Al, *Arabidopsis lyrata* subsp. *Lyrata* (XP_002873613.1); At, *Arabidopsis thaliana* (NP_568288.1); Pt, *Populus trichocarpa* (XP_002304638.1); Rc, *Ricinus communis* (XP_002512673.1); Vv, *Vitis vinifera* (XP_002271311.1); St, *Solanum tuberosum* (ABA81878.1); Os, *Oryza sativa Japonica Group* (NP_001046975.1); Zm, *Zea mays* (NP_001131229.1); Mt, *Medicago truncatula* (XP_003624512.1).

BcRISP1 was closely related to *Brassica rapa* ssp. *pekinensis* (Bra006199) and shares 96% similarity; the ubiquinol–cytochrome c reductase iron–sulfur subunit protein from *Arabidopsis lyrata* subsp. lyrata (XP_002873613.1), *Arabidopsis thaliana* (NP_ 568288.1) and *Populus trichocarpa* (XP_002304638.1) shared 91, 90 and 75% identity, respectively (Figure 1b).

Analysis of *BcRISP1* expression
qRT-PCR was used to compare *BcRISP1* expression between the sterile and maintainer lines at different flower developmental stages. There was a significant increase in the *BcRISP1* transcript in the sterile line at the archesporial cell stage compared with the maintainer line. At other periods of bud development, and in leaf tissues, no important differences in expression levels were observed between the sterile and maintainer lines (Figure 2).

Expression analysis of mitochondrial respiratory chain-related genes and biochemical assays of mitochondria in transgenic *Arabidopsis*
The expression pattern of the *BcRISP1* gene is shown in Figure 3a. The *BcRISP1* transcript was significantly higher in the three transgenic lines than in the wild-type plants throughout the entire growth cycle. Theoretically, ROS changes could occur when the mitochondria become dysfunctional in terms of electron transport.[20] We compared the ROS content in purified mitochondria from transgenic and wild-type plants. The ROS content in 35S::*BcRISP1* buds was 36.5% higher than in wild-type buds (Figure 3b). qRT-PCR assays were used to investigate the relationship between the overexpression of *BcRISP1* and members of the mitochondrial respiratory chain. *COX10*, which plays a critical role in the mitochondrial heme biosynthetic pathway,[21,22] and the QCR7 protein have been implicated in the proton conducting pathway from the matrix to the redox center of cytochrome b.[23] *SDH2-1* acts as a conductor of electrons from the flavoprotein to the membrane.[24] The expression levels of these genes were compared at different developmental stages in the transgenic and wild-type plants using qRT-PCR. The results revealed that the homologs of these genes were downregulated in 35S::*BcRISP1* plants compared with wild-type plants at the vegetative stage. However, at the generative growth stages, the expression levels of the *COX10* (At2g44520) and *RIP1* (At5g13440) homologs showed higher levels in 35S::*BcRISP1* plants than in the wild-type plants, whereas the *QCR7* (At4g32470) and *SDH2-1* (At3g27380) homologs showed

Figure 2. Expression levels of the *BcRISP1* gene during bud development in non-heading Chinese cabbage. M_1, M_2, M_3 and M_4 maintainer buds at different sizes (<0.5, 1.5, 2.5 and >3.5 mm), M_5 maintainer leaves; S_1, S_2, S_3 and S_4 Pol CMS buds at different sizes (<0.6, 1.8, 3.0 and >4.5 mm), S_5 maintainer leaves. Poly(A)$^+$-mRNA was isolated from buds at different development stages, converted to cDNA and quantified by qRT-PCR. Each data point represents mean±s.e. (n=3).

lower expression levels in the 35S::*BcRISP1* plants than in the wild-type plants (Figure 3c). This indicated that *BcRISP1* regulates mitochondrial electron transport associated genes in the 35S::*BcRISP1* overexpression lines.

Phenotypic analysis of transgenic *Arabidopsis*
No morphological differences were observed between 35S::*BcRISP1* and wild-type *Arabidopsis* plants during plant vegetative development. However, at flowering, the pistil was surrounded by shorter filaments and smaller anthers in the 35S::*BcRISP1* flowers (Figure 4a). Furthermore, 35S::*BcRISP1* plants had shorter siliques and a lower seed set than wild-type plants (Figure 4b and 4c). The 35S::*BcRISP1* lines produced fewer siliques compared with the wild-type plants (Figure 4d and 4e). The comparison of silique size and seed number between the 35S::*BcRISP1* and wild-type lines revealed that *BcRISP1* overexpression affected plant reproduction (Figure 4f and 4g).

Effects on the formation of pollen and the retarded growth of pollen tubes in transgenic plants
Regarding the reduced seed set observed in the *35S::BcRISP1* plants, we speculated whether this reduction was caused by pollen formation ability and/or the rate of pollen tube growth. The total number of pollen grains in the anthers from *35S::BcRISP1* plants was less than one-third of that observed in wild-type plants (Figure 5a–5c). To evaluate the *in vitro* pollen germination abilities, wild-type and *35S::BcRISP1* pollen was applied to agarose pads and cultivated for 4 h in a humid chamber. While wild-type pollen demonstrated 92.5% germination, the 35S::*BcRISP1* pollen exhibited only 63.9% germination (Figure 5d–5f). These findings suggest that *BcRISP1* expression in transgenic plants severely reduces the formation of normal pollen and impairs pollen tube growth.

DISCUSSION
In plant growth and development processes, mitochondrial function and activity are constantly changing.[25] The most compelling evidence for an essential role of mitochondria during pollen development is the phenomenon of CMS. Respiration is the core process of mitochondrial metabolism, with a large amount of free energy released and used for ATP production. Microsporogenesis is a high energy-demanding process that may impose stress on anther development.[26] The *BcRISP1* protein contains a Rieske [2Fe–2S] domain (Figure 1), which is a complex part of the electron transport chain in mitochondria. As microspores only have undifferentiated plastids and amyloplasts, the energy required for pollen development in the form of ATP must be supplied by mitochondria.[8] In non-heading Chinese cabbage CMS lines, anther development was inhibited at the archesporium cell stage, in which the flower size is smaller than 0.5 mm, and no anther sac was formed to produce normal sporogenous cells.[27] Our results revealed enhanced expression of BcRISP1 protein at the archesporial cell stage in the sterile line (Figure 2); this may inevitably cause electron transfer disorders and affect the normal energy supply in mitochondria. These results suggest that the central role of *BcRISP1* in mitochondrial electron transport and energy production has a key effect on the production of microspores and the formation of anthers. Mitochondrial Rieske iron–sulfur protein cloned from tobacco senses and responds to changes in energy metabolism and/or changes in mitochondrion numbers.[8] However, there was no indication of male sterility and reduced seed set as found in our study based on the abnormal expression of *BcRISP1* that could cause anthers to abort.

The nuclear-encoded mitochondrial RISP gene has been cloned and characterized in several species. In many organisms studied, the mitochondrial *RISP* is encoded by a single gene, while the mitochondrial *RISP* in tobacco is encoded by a small gene family, which can be divided into three subfamilies.[8] The mitochondrial *RISP* of
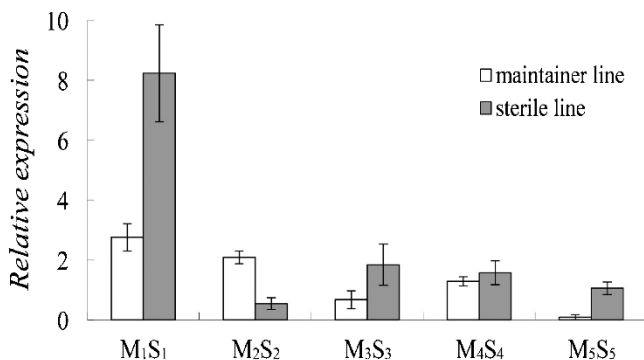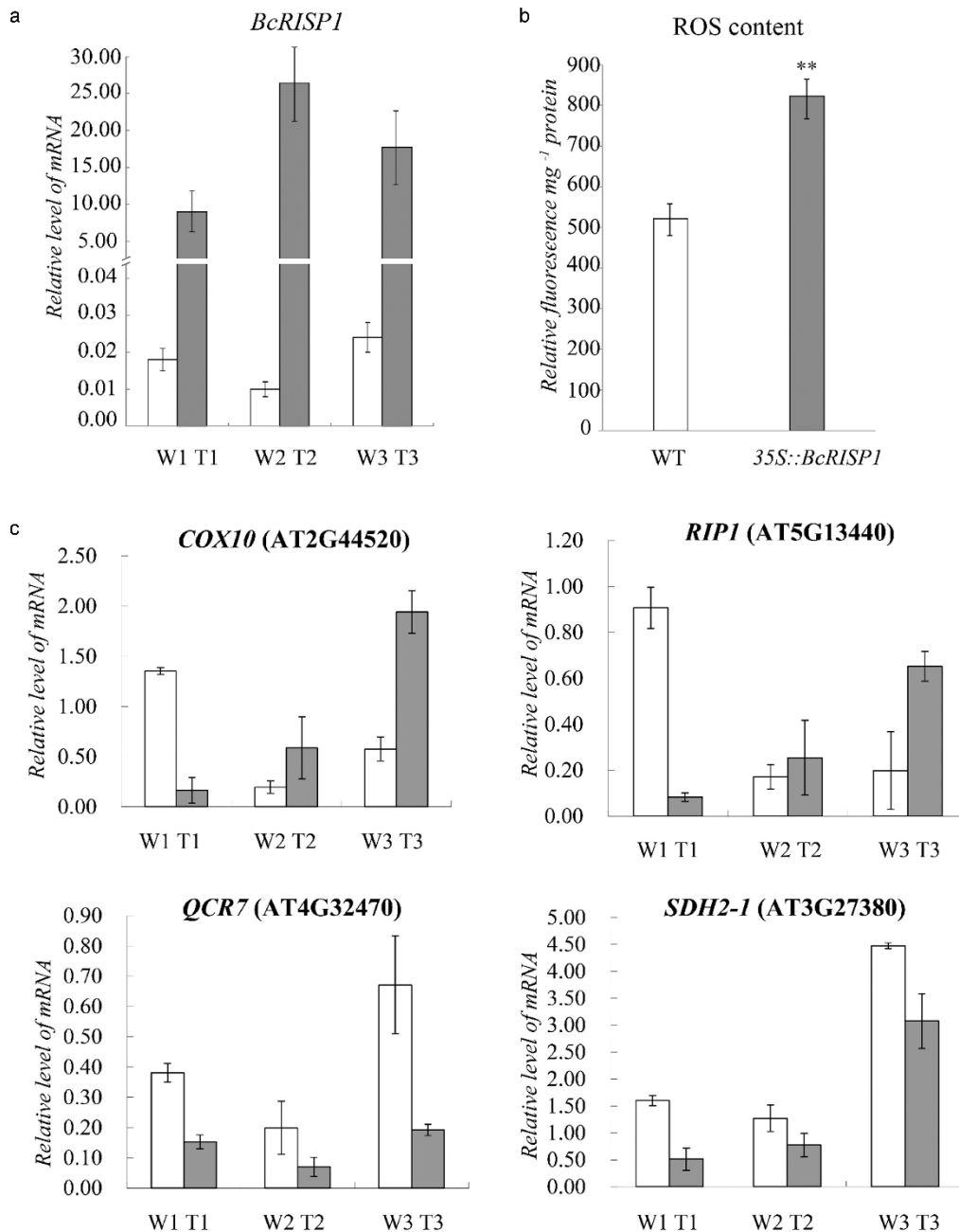
Figure 3. Effects of *BcRISP1* on mitochondrial respiratory chain-related gene expression. (**a**) *BcRISP1* expression levels in wild-type and 35S::*BcRISP1 Arabidopsis*. (**b**) ROS content of mitochondria in 35S::*BcRISP1 Arabidopsis* buds. All tests used equivalent mitochondrial quantities and were repeated three times. Significantly different from wild type at *$P<0.05$. The results are expressed as averages±s.d. (**c**) Expression levels of *COX10* (At2g44520), *RIP1* (At5g13440), *QCR7* (At4g32470) and *SDH2-1* (At3g27380) in wild-type and 35S::*BcRISP1 Arabidopsis* as determined by qRT-PCR. W1, W2 and W3, wild-type plants at vegetative, bolting and flowering stages, respectively; T1, T2 and T3, transgenic plants at vegetative, bolting and flowering stages, respectively. Error bars represent s.d. in three transgenic plants.

Chinese cabbage contains 12 members. The fact that disruption of the mitochondrial electron transport chain in 35S::*BcRISP1* overexpression lines did not cause male sterility may be caused by the gene expression disorder being masked by the function of other family members.

Cytoplasmic male sterility in plants is characterized by their inability to produce functional pollen. *SDH2-1* transcript accumulation in the anther is consistent with an essential role of mitochondria during anther development.[24] In this study, the expression level of

BcRISP1 was significantly increased in transgenic *35S::BcRISP1 Arabidopsis* plants (Figure 3a). *SDH2-1* had the highest mRNA expression levels in flowers[28] and was downregulated in 35S::*BcRISP1* overexpression lines compared to the wild-type (Figure 3c). This may be why some transgenic *Arabidopsis* plants produced anthers with few or no pollen.[29] The homolog of *RIP1* in *Arabidopsis* was downregulated at the vegetative growth stage, whereas *RIP1* was unregulated in the 35S::*BcRISP1* overexpression lines at the reproductive growth stage, which would consume more
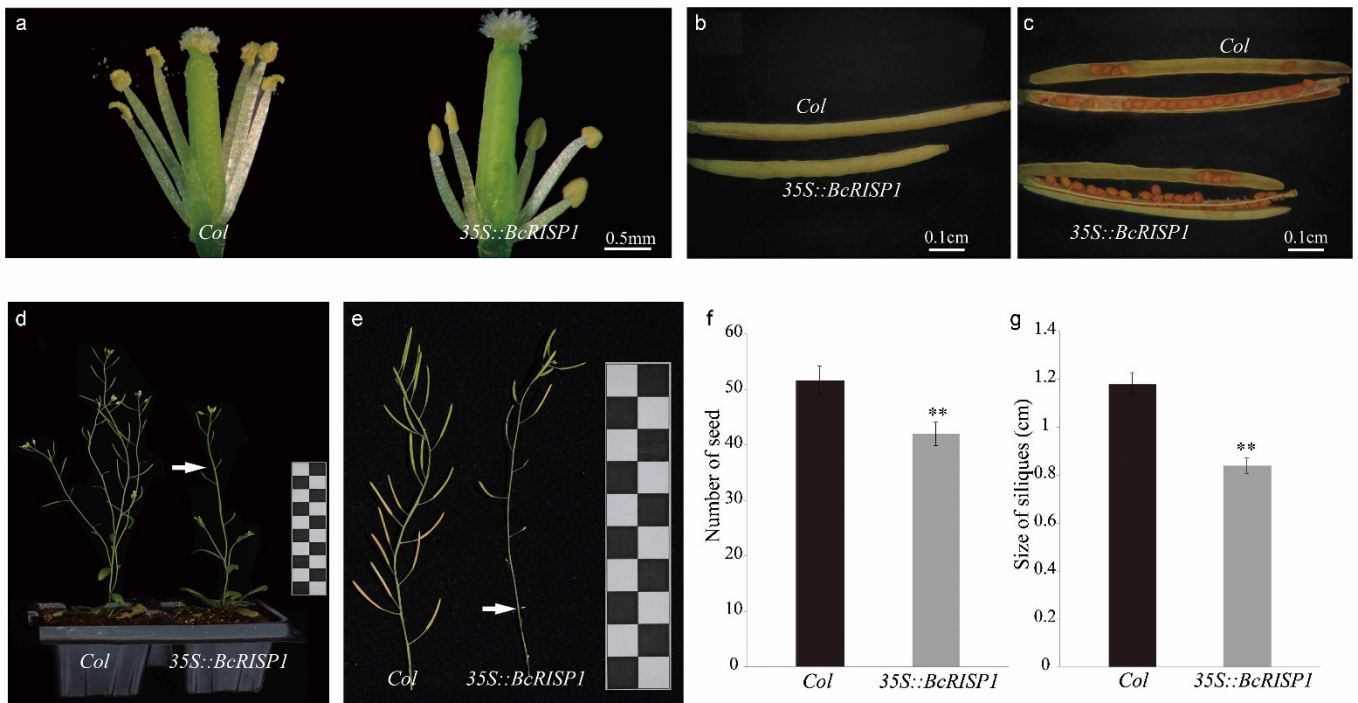
Figure 4. Flower and fruit phenotypes in wild-type and 35S::BcRISP1 *Arabidopsis* plants. (**a**) Detailed view of wild-type and 35S::*BcRISP1* flowers at a similar developmental stage with sepals and petals removed. (**b**) Wild-type and 35S::*BcRISP1* siliques. (**c**) Opened mature wild-type and 35S::*BcRISP1* siliques. (**d**) Whole plant wild-type and 35S::*BcRISP1* phenotypes. (**e**) Apical part of the main inflorescence stem from wild-type and 35S::*BcRISP1* plants. (**f**) Comparison of silique size between wild-type and 35S::*BcRISP1*. (**g**) Comparison of seed number between wild-type and 35S::*BcRISP1*. Significantly different from wild-type at *$P<0.05$. The results are expressed as averages±s.d. in three transgenic plants. Values represent means±s.e. ($n=10$) in three transgenic plants.
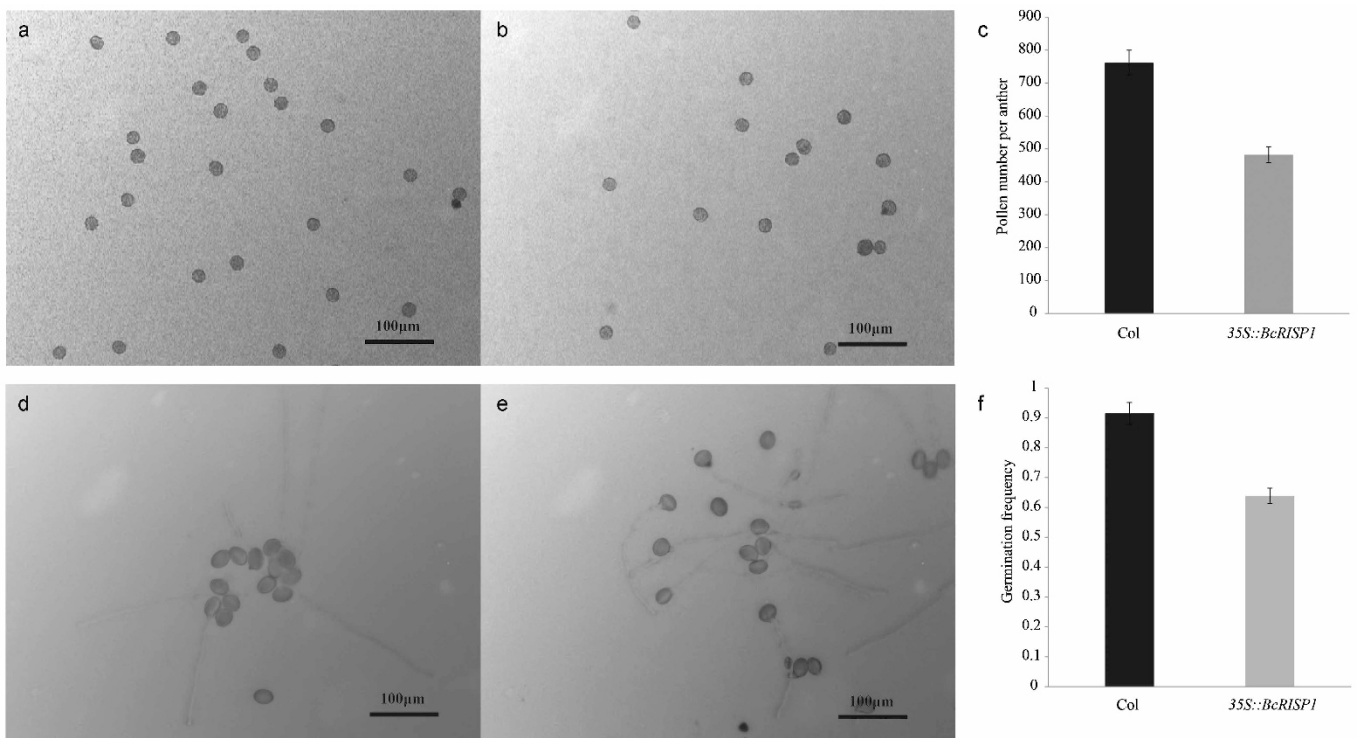
Figure 5. Phenotypic characterization of pollen produced from transgenic and wild-type *Arabidopsis* plants. (**a**) Pollen grains from wild-type plants stained with TTC solution. (**b**) Pollen grains from 35S::*BcRISP1* plants stained with TTC solution. (**c**) Total numbers of pollen grains in an anther from wild-type and 35S::*BcRISP1* plants. (**d**) *In vitro* germination of pollen from wild-type plants. (**e**) *In vitro* germination of pollen from 35S::*BcRISP1* plants. (**f**) Germination rates of pollen grains from wild-type and 35S::*BcRISP1* plants. Results are given as averages±s.d.

electrons for the reduction of cytochrome c (Figure 3c). As feedback inhibitors, the expression levels of the two upstream genes, *SDH2-1* and *QCR7*, should be decreased; this was confirmed by the analysis (Figure 3c). Conversely, the downstream gene *COX10* was upregulated and accompanied the overexpression of *BcRISP1* to catalyze the transfer of electrons from reduced cytochrome c to molecular oxygen;[6] this caused disruption of the mitochondrial electron transport chain because less electrons were produced due to the low expression of the upstream genes. The complex III of the electron transport chain is a principal source of ROS, and the inhibition of cytochrome c reductase activity increases ROS generation and oxidative damage.[30] Defects in supercomplex function, such as the absence of RISP, can cause increased levels of ROS at the mitochondrial inner membrane.[31] Hence, we inferred that complex III produced more ROS (Figure 3b) in 35S::*BcRISP1* lines as a result of electron transport chain dysfunction. CMS protein ORFH 79 binds to electron transport chain complex III, causing increased ROS and reduced ATP concentration, ultimately leading to the pollen abortion.[16] Overall, the observed expression changes in the mRNA levels within the 35S::*BcRISP1* overexpression lines indicated that *BcRISP1* affected mitochondrial energy metabolism, leading to an abnormal mitochondrial respiratory chain with increased ROS generation, which may explain the reduced seed set phenotypes observed in transgenic plants.

The protein BLAST search revealed that ubiquinol–cytochrome c reductase iron–sulfur subunit *BcRISP1* had several homologs in plants (Figure 1b). One homolog from *Arabidopsis* (TAIR: At5g13430) was reported to change significantly during pollen germination and tube growth,[32] which is an essential process for the reproduction of flowering plants. Pollen tubes are an excellent model for investigating the contribution of respiration to plant cellular growth, with full-on energy-generating respiration, which is very important to the pollen tube.[33] Drastic retardation of pollen tube growth and impaired pollen tube guidance and reception can lead to disruption of fertilization and seed development.[34] Suppression subtractive hybridization revealed that *BcRISP1* was highly expressed in the male sterile line (Pol CMS) of non-heading Chinese cabbage (data not shown). However, this significant characteristic of sterility was not observed in transgenic *Arabidopsis*, whereas the phenomena of reduced pollen formation and impaired pollen tube growth were observed in transgenic *Arabidopsis* (Figure 5). Furthermore, compared with the wild-type, fewer seeds and smaller siliques were found in the 35S::*BcRISP1* lines (Figure 4). This result indicates that fertility is reduced in the transgenic lines. We suggest that the lower seed set could be due to the overexpression of *BcRISP1*, which disrupted the mitochondrial electronic chain and impaired the development of anthers.

COMPETING INTERESTS
The authors declare no conflict of interest.

REFERENCES
1 Lee SJ, Warmke HE. Organelle size and number in fertile and T-cytoplasmic male-sterile corn. *Am J Bot* 1979; **60**: 141–148.

2 Goldberg RB, Beals TP, Sanders PM. Anther development: basic principles and practical applications. *Plant Cell* 1993; **5**: 1217–1229.

3 McCormick S. Control of male gametophyte development. *Plant Cell* 2004; **16**: 142–153.

4 Scott RJ, Spielman M, Dickinson HG. Stamen structure and function. *Plant Cell* 2004; **16**: 46–60.

5 Paepe AD, Leroy JG, Nuytinck L, Meire F, Capoen J. Osteoporosis-pseudoglioma syndrome. *Am J Med Genet* 1993; **4**: 530–537.

6 Hanson MR, Bentolila S. Interactions of mitochondrial and nuclear genes that affect male gametophyte development. *Plant Cell* 2004; **16**: 154–169.

7 Davidson E, Ohnishi T, Atta-Asafo-Adjei E, Daldal F. Potential ligands to the [2Fe–2S] Rieske cluster of the cytochrome bc1 complex of *Rhodobacter capsulatus* probed by site-directed mutagenesis. *Biochemistry* 1992; **31**: 3342–3351.

8 Huang J, Struck F, Matzinger DF, Levings CS. Flower-enhanced expression of a nuclear-encoded mitochondrial respiratory protein is associated with changes in mitochondrion number. *Plant Cell* 1994; **6**: 439–448.

9 Trumpower BL, Gennis RB. Energy transduction by cytochrome complexes in mitochondrial and bacterial respiration: the enzymology of coupling electron transfer reactions to transmembrane proton translocation. *Annu Rev Biochem* 1994; **63**: 675–716.

10 Trumpower BL, Edwards CA. Purification of a reconstitutively active iron–sulfur protein (oxidation-factor) from succinate–cytochrome c reductase complex of bovine heart mitochondria. *J Biol Chem* 1979; **254**: 8697–8706.

11 Beckmann JD, Ljungdahl PO, Lopez JL, Trumpower BL. Isolation and characterization of the nuclear gene encoding the Rieske iron–sulfur protein (RIP1) from *Sacchammyces cerevisiae*. *J Biol Chem* 1987; **262**: 8901–8909.

12 Laser KD, Lersten NR. Anatomy and cytology of microsporogenesis in cytoplasmic male sterile angiosperms. *Bot Rev* 1972; **38**: 427–454.

13 Li GH, Zhang YR, Cao J, Li G. [Application of heterosis of male sterility on cruciferous vegetables.] *Acta Agric Univ Jiangxiensis* 2003; **25**: 181–186. Chinese.

14 Livak KJ, Schmittgen TD. Analysis of relative gene expression data using real-time quantitative PCR and the $2^{-\Delta\Delta C_T}$ method. *Methods* 2001; **25**: 402–408.

15 Liu TK, Li Y, Zhang CW, Qian Y, Wang Z, Hou XL. Overexpression of FLOWERING LOCUS C, isolated from Non-heading Chinese cabbage (*Brassica campestris* ssp. *chinensis* Makino), influences fertility in *Arabidopsis*. *Plant Mol Biol Rep* 2012; **6**: 1444–1449.

16 Wang K, Gao F, Ji YX. ORFH79 impairs mitochondrial function via interaction with a subunit of electron transport chain complex III in Honglian cytoplasmic male sterile rice. *New Phytologist* 2013; **198**: 408–418.

17 Iwata S, Lee JW, Okada K *et al*. Complete structure of the 11-subunit bovine mitochondrial cytochrome bc1 complex. *Science* 1998; **281**: 64–71.

18 Harnisch U, Weiss H, Sebald W. The primary structure of the iron-sulfur subunit of ubiquinol-cytochrome c reductase from *Neurospora*, determined by cDNA and gene sequencing. *Eur J Biochem* 1985; **149**: 95–99.

19 Madueño F, Napier JA, Cejudo FJ, Gray JC. Import and processing of the precursor of the Rieske FeS protein of tobacco chloroplasts. *Plant Mol Biol* 1992; **20**: 289–299.

20 Moller IM, Sweetlove LJ. ROS signalling-specificity is required. *Trends Plant Sci* 2010; **15**: 370–374.

21 Barros MH, Carlson CG, Glerum DM, Tzagoloff A. Involvement of mitochondrial ferredoxin and Cox15p in hydroxylation of heme O. *FEBS Lett* 2001; **492**: 133–138.

22 Barros MH, Nobrega FG, Tzagoloff A. Mitochondrial ferredoxin is required for heme A synthesis in *Saccharomyces cerevisiae*. *J Biol Chem* 2002; **277**: 9997–10002.

23 Lorusso M, Cocco T, Boffoli D, Meinhardt S, Ohnishi T, Papa S. Effect of papain digestion on polypeptide subunits and electron-transfer pathways in mitochondrial b–c1 complex. *Eur J Biochem* 1989; **179**: 535–540.

24 Elorza A, León G, Gómez I. Nuclear *SDH2-1* and *SDH2-2* genes, encoding the iron-sulfur subunit of mitochondrial complex II in *Arabidopsis*, have distinct cell-specific expression patterns and promoter activities. *Plant Physiol* 2004; **136**: 4072–4087.

25 Millar AH, Whelan J, Soole KL, Day DA. Organization and regulation of mitochondrial respiration in plants. *Annu Rev Plant Biol* 2011; **62**: 79–104.

26 Warmke HE, Lee SL. Pollen abortion in T cytoplasmic male-sterile corn (*Zea mays*): a suggested mechanism. *Science* 1978; **200**: 561–563.

27 Yang XY, Cao SC. [Cytomorphological research on anther development of Pol CMS in non-heading Chinese cabbage (*Brassica campestris*. ssp.*chinensis* Makino).] *J Nanjing Agric Univ* 1997; **20**: 36–43. Chinese.

28 Figueroa P, León G, Elorza A, Holuigue L, Jordana X. Three different genes encode the iron-sulfur subunit of succinate dehydrogenase in *Arabidopsis thaliana*. *Plant Mol Biol* 2001; **46**: 241–250.

29 Hepworth SR, Valverde F, Ravenscroft D, Mouradov A, Coupland G. Antagonistic regulation of flowering-time gene *SOC1* by CONSTANS and FLC via separate promoter motifs. *EMBO J* 2002; **21**: 4327–4337.

30 Chen Q, Vazquez EJ, Moghaddas S, Hoppel CL, Lesnefsky EJ. Production of reactive oxygen species by mitochondria: central role of complex III. *J Biol Chem* 2003; **278**: 36027–36031.

31 Diaz F, Enríquez JA, Moraes CT. Cells lacking Rieske iron–sulfur protein have a reactive oxygen species-associated decrease in respiratory complexes I and IV. *Mol Cell Biol* 2012; **32**: 415–429.

32 Wang Y, Zhang WZ, Song LF. Transcriptome analyses show changes in gene expression to accompany pollen germination and tube growth in *Arabidopsis*. *Plant Physiol* 2008; **148**: 1201–1211.

33 Rounds CM, Winship LJ, Hepler PK. Pollen tube energetics: respiration, fermentation and the race to the ovule. *AoB Plants* 2011; **19**: 1–14.

34 Zhou JJ, Liang Y, Niu QK, Chen LQ, Zhang XQ, Ye D. The *Arabidopsis* general transcription factor TFIIB1 (*AtTFIIB1*) is required for pollen tube growth and endosperm development. *J Exp Bot* 2013; **64**: 2205–2218.